



UNIVERSITY OF LEEDS

This is a repository copy of *Investigation into intermodulation distortion in HEMTs using a quasi-2-D physical model* .

White Rose Research Online URL for this paper:
<http://eprints.whiterose.ac.uk/719/>

Article:

Rudge, P.J., Miles, R.E., Steer, M.B. et al. (1 more author) (2001) Investigation into intermodulation distortion in HEMTs using a quasi-2-D physical model. *IEEE Transactions on Microwave Theory and Techniques*, 49 (12). pp. 2315-2321. ISSN 0018-9480

<https://doi.org/10.1109/22.971615>

Reuse

See Attached

Takedown

If you consider content in White Rose Research Online to be in breach of UK law, please notify us by emailing eprints@whiterose.ac.uk including the URL of the record and the reason for the withdrawal request.



eprints@whiterose.ac.uk
<https://eprints.whiterose.ac.uk/>

Investigation Into Intermodulation Distortion in HEMTs Using a Quasi-2-D Physical Model

Peter J. Rudge, Robert E. Miles, Michael B. Steer, *Fellow, IEEE*, and Christopher M. Snowden, *Fellow, IEEE*

Abstract—The need for both linear and efficient pseudomorphic high electron-mobility transistors (pHEMTs) for modern wireless handsets necessitates a thorough understanding of the origins of intermodulation distortion at the device level. For the first time, the dynamic large-signal internal physical behavior of a pHEMT is examined using a quasi-two-dimensional physical device model. The model accounts fully for device-circuit interaction and is validated experimentally for a two-tone experiment around 5 GHz.

Index Terms—Intermodulation distortion, linearity, microwave power FET amplifiers, MODFET power amplifiers, MODFETs, semiconductor device modeling.

I. INTRODUCTION

THE requirement of linear performance is particularly critical in digital radio where spectral regrowth and in-band distortion are factors which limit performance. There is an inherent tradeoff between maximizing efficiency and minimizing spectral regrowth and in-band distortion. Large-signal peak-to-average ratios mean that amplifiers must have good intermodulation performance. For wireless handsets, issues of cost, size, and complexity limit the extent to which predistortion and feed-forward linearization can be used. An alternative to this is to optimize device structures for low intermodulation distortion (IMD). The work presented here provides detailed insight into the dynamic large-signal internal physical behavior of high electron-mobility transistors (HEMTs). This behavior cannot be accounted for by quasi-static large-signal equivalent-circuit models.

Equivalent-circuit-based models are commonly used to investigate large-signal device performance. However, these models require extensive characterization of the device after fabrication, as well as some knowledge of process variation statistics. For the well-proven physical model used here, there is no need for an extensive series of measurements since all the data are provided from the process parameters and physical structure of the device. Equivalent-circuit models also suffer from problems associated with curve-fitting errors and discontinuous or inaccurate high-order derivatives in current and voltage expressions, leading to inaccurate predictions of IMD. Physical models solve the semiconductor equations explicitly for the device and avoid

the problem of ill-defined relationships between equivalent-circuit elements and physical behavior.

In the past, equivalent-circuit-based models (such as the Root model [1]) have, using the physical model, been extracted from multibias S -parameter simulations in order to examine large-signal behavior [2]–[5]. The present paper extends this previous work by embedding the device model directly in a circuit to account fully for device–circuit interactions. The simulations run on circuit computer-aided design (CAD) time scales allowing two-tone performance to be assessed for a particular device structure prior to fabrication. Internal device behavior (in terms of electric field, charge, etc.) is examined and related to global device–circuit performance. By these means it is possible to evaluate quantitatively the impact of device structure, biasing, and loading on device performance and optimize device structure and operation for optimum linearity performance and efficiency. This is critical in modern wireless mobile communications. To the authors' knowledge, this is the first time that dynamic large-signal data on internal physical device behavior derived from a physical model have been presented. We believe that this is the first step in optimizing device epitaxy, geometry, and operating conditions for the best combination of distortion performance and efficiency. Our ultimate goal is to relate low-level device characteristics to system-level performance parameters such as spectral regrowth, in-band distortion, and bit error rate (BER) [6].

II. PHYSICAL MODEL

The pseudomorphic high-electron mobility (pHEMT) model utilizes a quasi-two-dimensional (Q2D) carrier transport description, which has previously been reported [2]–[5], [7], [8]. The model requires a description of the geometry and epitaxy of the device and has been used to successfully predict dc, S -parameter, and large-signal performance. Thermal effects are also included. The Q2D model is based on a simplified solution of the hot electron hydrodynamic transport model given here as

$$\frac{\partial n}{\partial t} + \nabla \cdot (nv) = 0 \quad (1)$$

$$\begin{aligned} \frac{\partial v}{\partial t} + \mathbf{v} \cdot \nabla v &= \frac{q}{m^*} \mathbf{E} - \frac{2}{3m^*n} \nabla (nv) \\ &+ \frac{1}{3n} \nabla (nv^2) - \frac{\mathbf{v}}{\tau_p} \end{aligned} \quad (2)$$

$$\begin{aligned} \frac{\partial w}{\partial t} + \mathbf{v} \cdot \nabla w &= q\mathbf{v} \cdot \mathbf{E} - \frac{2}{3n} \nabla \cdot \left[n\mathbf{v} \left(w - \frac{m^*}{2} v^2 \right) \right] \\ &- \frac{1}{n} \nabla \cdot \mathbf{Q} - \frac{w - w_0}{\tau_w}. \end{aligned} \quad (3)$$

Manuscript received March 30, 2001; revised August 21, 2001. This work was supported by M/A-COM Corporate Research and Development.

P. J. Rudge, R. E. Miles, and C. M. Snowden are with the Institute of Microwaves and Photonics, School of Electronic and Electrical Engineering, The University of Leeds, Leeds LS2 9JT, U.K. (e-mail: p.j.rudge@ieee.org).

M. B. Steer is with the Department of Electrical and Computer Engineering, North Carolina State University, Raleigh, NC 27695-7914 USA.

Publisher Item Identifier S 0018-9480(01)10463-1.

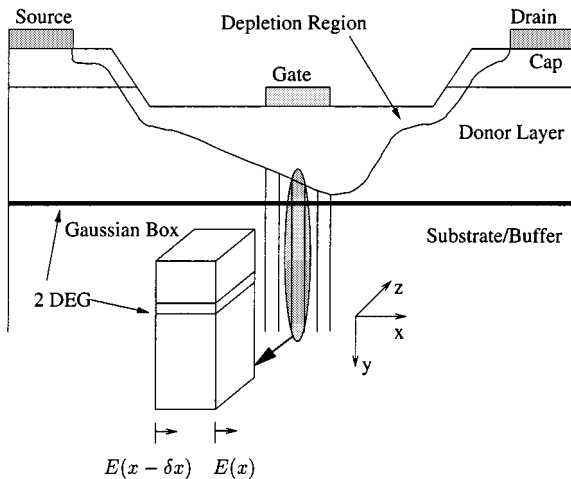


Fig. 1. Q2D approach to HEMT modeling.

These equations represent particle, momentum, and energy conservation, respectively [2], [7]. The model assumes that carrier transport takes place primarily in a plane parallel to the device surface [8]. This assumption is based on results from full two-dimensional (2-D) simulations, which show that equipotential lines in the undepleted part of the HEMT active channel are almost parallel. This approach has been validated with respect to both measurements and Monte Carlo simulations [8]. A schematic of the Q2D approach to modeling a typical device is shown in Fig. 1.

The transport model includes current continuity, energy, and momentum equations, allowing us to account for hot electron effects. The suitability of the type of transport model used here for the rapidly changing fields involved in large-signal device operation is discussed in [9]. The charge-control model includes quantum effects and accounts for trapping and injection of electrons into the buffer. Buffer injection is treated by means of a separate, but coupled, analytical model [10].

The charge-control model is implemented via a series of Gaussian boxes along the channel, as illustrated in Fig. 1. For each Gaussian box, the Poisson and one-dimensional (1-D) Schrodinger equations are solved self-consistently to determine the charge within the box. This is done under a range of conditions and the data stored in a charge-control lookup table. This calculation is time-consuming but only needs to be performed once for a given epitaxial layer structure. The terminal voltages and currents are obtained by stepping along the channel from source to drain and solving the transport equations self-consistently with the charge-control data in the lookup table. In spite of the Q2D nature of the model, 2-D charge control is retained and the simulation runs over 1000 times faster than full 2-D models. More background on the Q2D approach to device modeling can be found in [3]–[5], and [8].

III. SIMULATIONS

To simulate device-circuit performance, the Q2D model was embedded in an external circuit model as shown in Fig. 2. The linear networks contain sources, loads, parasitic element networks, and bias circuitry. The linear networks were modeled by forming second-order linear differential nodal current and

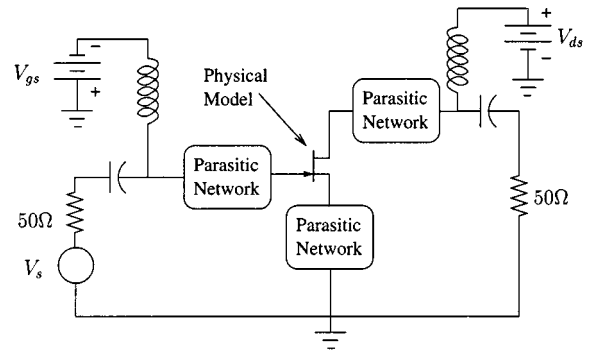


Fig. 2. Schematic of the device-circuit simulation.

voltage equations. These were then discretized in the time domain and the resulting set of simultaneous linear equations solved using Gaussian elimination. The derivatives of the currents and voltages in the linear networks were calculated using a simple backward difference scheme. The trapezoidal method was employed to evaluate integrals.

In order to account for device-circuit interaction, the Q2D model equations were solved self-consistently with those of the linear networks using a Newton–Raphson scheme. Careful attention was paid to the size of the time step used to ensure an efficient and stable solution. Large time steps were used for the first few time points. The time step size is subsequently reduced as the simulation progresses. It was found that this approach is most suitable to enable the solution to converge rapidly.

Care must be taken in choosing the resolution of the charge-control lookup table. A coarse mesh results in “spikes” in the currents and voltages at the device terminals for large signals. This is due to the fact that a large signal will traverse a greater range of the lookup table than a small signal. On the other hand, a very fine mesh is expensive in terms of simulation time and data storage.

Convergence is rapid, with simulations taking, on average, 0.6 CPU s per time point on a 450-MHz Pentium III workstation with 64 Mb of RAM. Steady state is reached typically within 100 time points.

IV. MODEL VALIDATION

In order to validate the model a six-finger double recessed pHEMT with 0.23- μm gate length and total gatewidth of 360 μm was measured and simulated. The device was terminated with 50- Ω source and load impedances and biased with $V_{ds} = 3$ V and $V_{gs} = -0.2$ V in class A configuration. Two-tone measurements and simulations were performed with tones at 4.75 GHz and 5.25 GHz. Fig. 3 shows the fundamental output power against available input power for the tone at 4.75 GHz. Excellent agreement is achieved, within 0.5 dB, through a broad range of input powers and into 4.5 dB of gain compression.

If we let $f_1 = 4.75$ GHz and $f_2 = 5.25$ GHz, it can be shown that the most significant distortion products for circuit designers are caused by third-order intermodulation products at $2f_2 - f_1$ (5.75 GHz) and $2f_1 - f_2$ (4.25 GHz), along with fifth-order products at $3f_2 - 2f_1$ (6.25 GHz) and $3f_1 - 2f_2$ (3.75 GHz) [11].

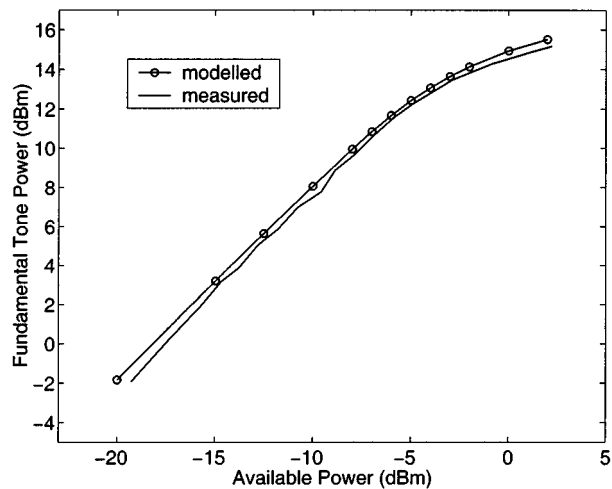


Fig. 3. Fundamental output power at 4.75 GHz against available input power for two-tone test with tones at 4.75 and 5.25 GHz.

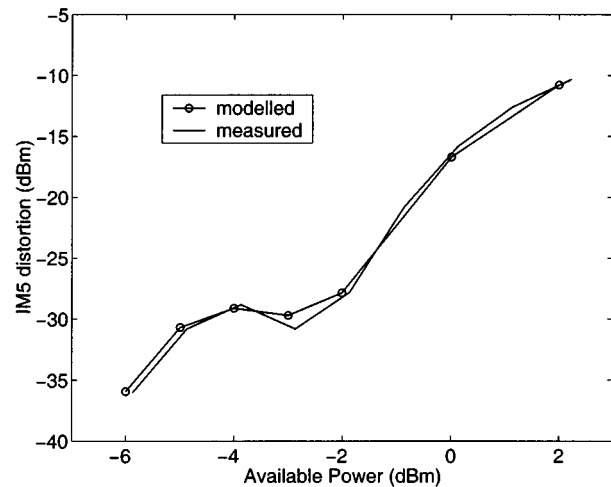


Fig. 5. Measured and modeled fifth-order IMD against available input power at $3f_2 - 2f_1 = 6.25$ GHz.

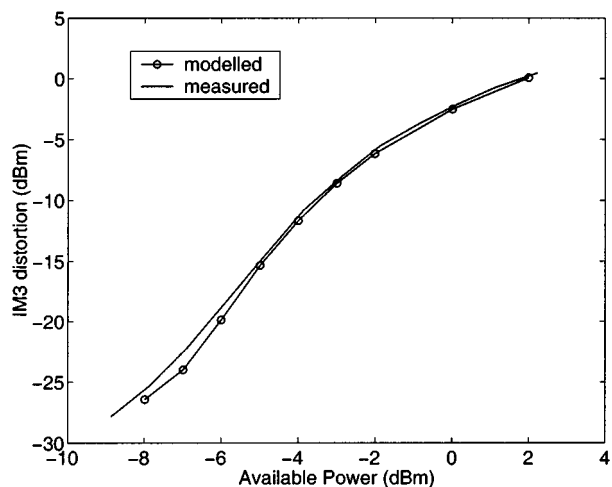


Fig. 4. Measured and modeled third-order IMD against available input power at $2f_2 - f_1 = 5.75$ GHz.

Fig. 4 shows third-order IMD results (data taken at 5.75 GHz). Modeled and measured results show excellent agreement. The two sets of results are within approximately 1 dB throughout the range of input powers but agreement is very good well into compression. Fig. 5 shows fifth-order distortion results (data taken at 6.25 GHz). Again, there is excellent agreement across the full range of input powers with a maximum discrepancy of around 1 dB. The results correspond especially well in the region of gain compression. The agreement between modeled and measured results across a range of powers and at significant frequencies was found to be excellent. Not only are they very close, but the general shape of the responses are remarkably similar. To the authors' knowledge, these represent some of the best multitone results obtained with either physically derived, empirical, or measurement-based models. The results suggest that phenomena that significantly affect large-signal performance (such as hot electron effects, gate conduction, trapping, etc.) are well modeled and that the physical model used here is suitable for

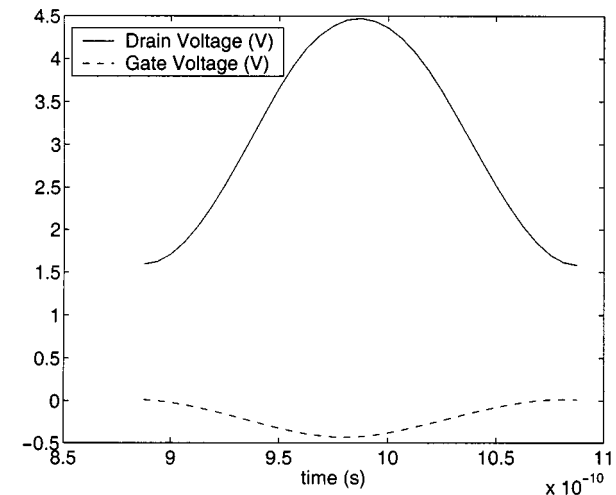


Fig. 6. Simulated terminal voltages for a signal before the onset of gain compression, corresponding to plots in Figs. 7–9.

large peak-to-average-ratio multitone simulations. It must be noted, however, that, in order to reduce simulation times, as short a time period as possible is simulated. This necessarily limits the dynamic range of the Fourier transforms used to calculate IMD. Thus, to uncover weakly nonlinear behavior, which may be significant in modern RF subsystems, simulation times would have to be increased.

V. PHYSICAL DEVICE ANALYSIS

In order to examine the internal physical behavior of the device under investigation, values for the electric field E , the channel electron sheet density N , and the electron concentration in the buffer N_{buff} , were extracted from the solution of the semiconductor equations. Each parameter is characterized as a function of time t and distance x along the channel. Fig. 6 shows the results of a sinusoidal excitation driving the device just below the onset of gain compression. Figs. 7–9 show plots of the device parameters as functions of x and t corresponding

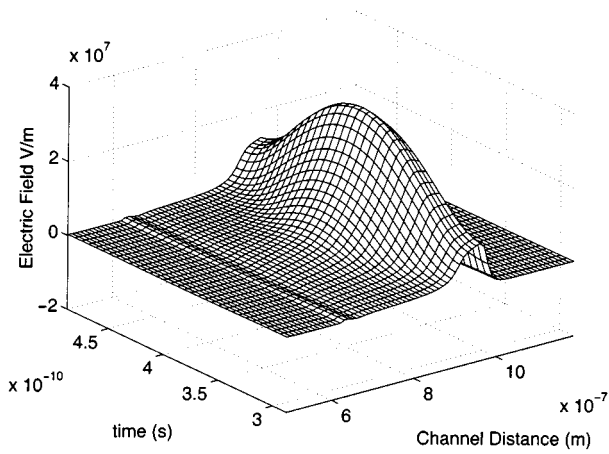


Fig. 7. Electric field as a function of channel distance and time for a signal before the onset of gain compression.

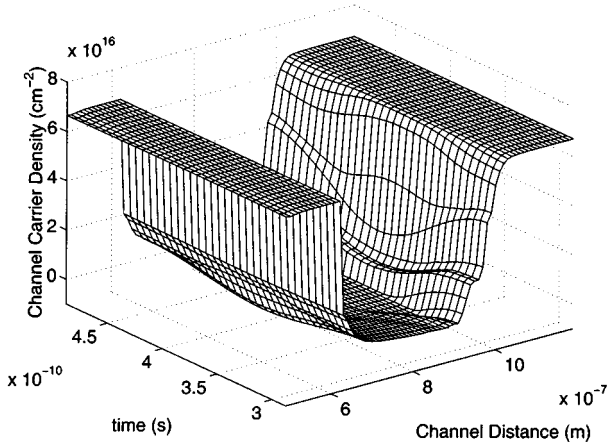


Fig. 8. Channel sheet carrier density as a function of channel distance and time for a signal before the onset of gain compression.

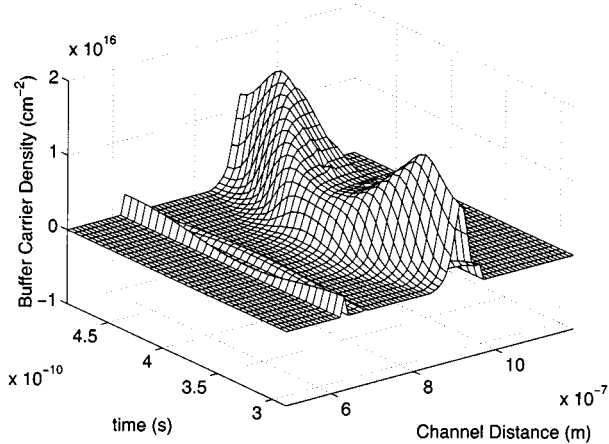


Fig. 9. Buffer carrier density as a function of channel distance and time for a signal before the onset of gain compression.

to the device terminal voltages shown in Fig. 6. The boundaries of the gate contact are at 0.69 and 0.91 μm . Only the region around the gate is shown as this is where most of the interesting charge-control effects in the device occur. In order to examine large-signal behavior, the channel profiles in Figs. 11–13 are presented. These are the results of driving the device with a

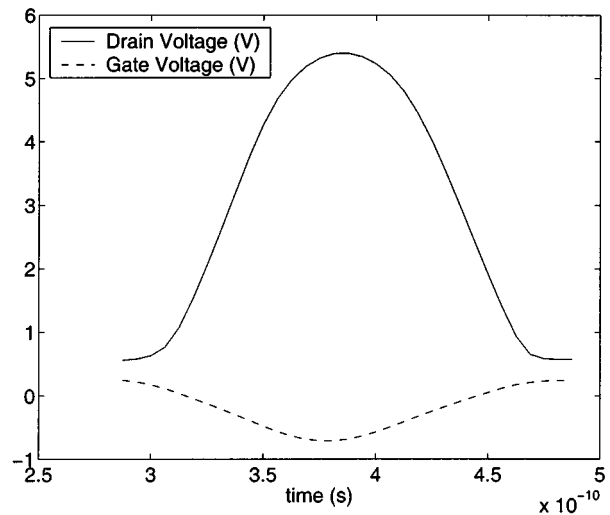


Fig. 10. Terminal voltages for a signal at 1-dB gain compression point, corresponding to plots in Figs. 11–13.

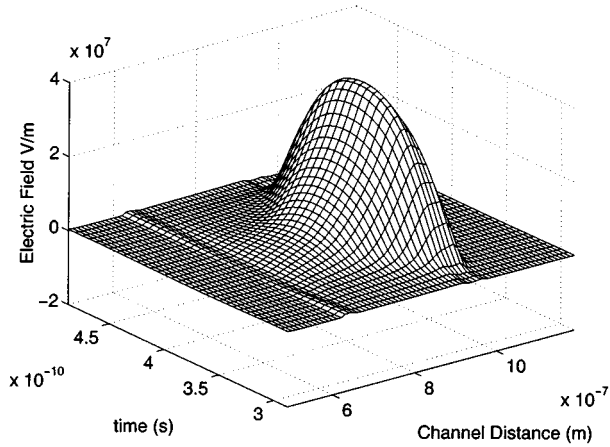


Fig. 11. Electric field as a function of channel distance and time for a signal at 1-dB gain compression point.

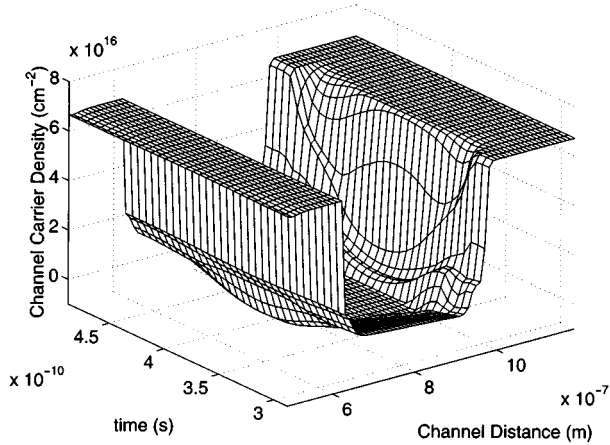


Fig. 12. Channel sheet carrier density as a function of channel distance and time for a signal at 1-dB gain compression point.

sinusoidal source into 1 dB of gain compression. The terminal voltages associated with these channel profiles are given in Fig. 10. There are several interesting points we can make about these plots.

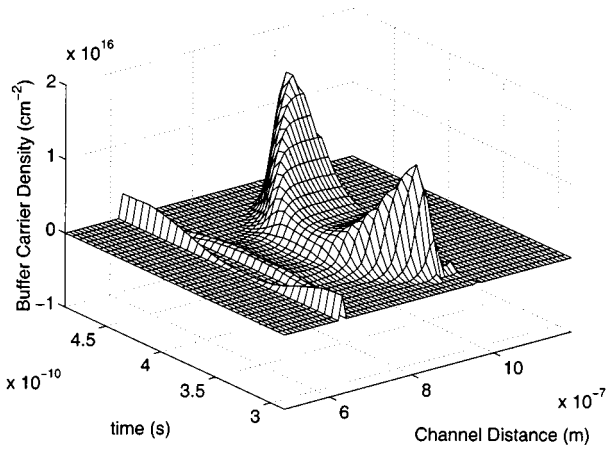


Fig. 13. Buffer carrier density as a function of channel distance and time for a signal at 1-dB gain compression point.

A. Electric Field E

Looking at the electric field plots in Figs. 7 and 11, we can see that, as expected, the electric field rises to a peak just beyond the drain edge of the gate and falls sharply again. Steeper gradients in both space and time are evident for the large-signal excitation.

B. Channel Electron Concentration

The channel electron concentration N is shown in Figs. 8 and 12. The effects of channel depletion are clear and coincide with large values of electric field. As expected, depletion is more pronounced at the drain edge of the gate. Another important effect is the increase in electron concentration at the drain edge of the gate in regions where the time and space derivatives of the electric field $\partial E/\partial t$ and $\partial E/\partial x$, respectively, are at their peaks. The contribution from $\partial E/\partial t$ to this is simply due to displacement current, i.e., capacitive effects. The contribution from $\partial E/\partial x$ can be explained by examination of the 2-D Poisson equation [2]

$$\frac{\partial E_y}{\partial y} + \frac{\partial E_x}{\partial x} = -\frac{\rho}{\epsilon} \quad (4)$$

where E_x and E_y are the x - and y -directed electric fields (x is parallel to the device surface and y is normal to it), ρ is the charge density, and ϵ is the permittivity. It can be seen that changes in $\partial E/\partial x$ result in changes in the charge density. Both these effects are more pronounced in the large-signal case due to the steeper field gradients involved.

The large-signal case shows pronounced channel depletion at the drain edge of the gate and, correspondingly, saturation of the 2 DEG channel is also evident.

C. Buffer Electron Concentration

Buffer electron concentration N_{buff} is shown in Figs. 9 and 13. These plots show dislocation of the 2 DEG layer by electron injection into the buffer. The same mechanism of large values of $\partial E/\partial x$ and $\partial E/\partial t$ is responsible for this phenomenon. It is interesting to note that the capacitive contribution to buffer injection is dominant. This behavior is not accounted for in quasi-static large-signal equivalent-circuit models. There is an interesting asymmetry in the waveform with the peak buffer

charge on the “falling edge” of the drain voltage being significantly larger than the peak charge on the “rising edge.” This effect becomes more pronounced the further into gain compression the device is driven. This can be explained by the fact that, when the device is driven into compression, the waveform becomes more and more asymmetrical, as can be seen in Fig. 10. Typically, the waveform widens on one half of the cycle whilst narrowing on the other half. This means that $\partial E/\partial t$ is different for the “rising” and “falling” edges of the drain voltage. It is also worth noting that the charge concentration in the “trough” between the two peaks becomes smaller as the device is driven into compression, again due to capacitive effects.

VI. CHANNEL PROFILES AND DISTORTION

One of the major causes of distortion in microwave field-effect transistors (FETs) is the nonlinear transconductance g_m . Transconductance drops for voltages close to pinchoff and gate-forward voltages around the onset of gate conduction. The reasons for the fall in g_m around pinchoff are the depletion of the 2 DEG layer of electrons and deconfinement of electrons from the quantum-well channel: electrons are injected from the channel into the buffer and contribute to channel current, but with a lower mobility than in the 2 DEG channel. These electrons are far from the gate so charge control, and hence transconductance, is reduced [12]. This can be interpreted as a shift in the effective position of the 2 DEG layer, which is dependent on the gate voltage, with a consequent nonlinear relationship between channel carrier concentration and gate voltage [13]

$$n_s = \frac{\epsilon}{q(d + \Delta d)} (V_G - V_T) \quad (5)$$

where n_s is the 2 DEG sheet charge density, d is the distance from the gate to the heterointerface, Δd is the effective position of the 2 DEG (which is dependent on gate bias), V_G is the gate voltage, and V_T the threshold voltage.

The transconductance falls around forward-bias gate voltages due to the onset of parallel conduction in the doped donor layer (AlGaAs in a conventional GaAs/AlGaAs HEMT) and saturation of the 2 DEG layer [12]. The build-up of charge in the (low mobility) donor layer shields the 2 DEG layer from the charge-control effects of the gate, thus reducing transconductance.

The idea of linearizing the transconductance with respect to gate voltage has been well explored in the case of metal-semiconductor FETs (MESFETs) [14]–[17]. Much less work has been reported on HEMT structures [18], [19]. Work on MESFETs has concentrated on tailoring the doping profile in the active layer such that charge control is linearized as compared with a uniform doping profile. The fact that forward-biased HEMTs form a parasitic MESFET in the doped donor layer means that tailoring the doping profile in HEMTs offers similar advantages. This is reflected in the improved linearity of delta-doped structures. Lour *et al.* have extended the concept by introducing delta-doping in the channel of pHEMTs [18]. Most approaches are based on rough approximations to the charge-control in the device. There are reports of HEMT devices

that have been fabricated with linearized dc transconductance, but to the authors' knowledge no large-signal data have been presented, which makes it difficult to assess the merits of the approach. Also, detailed analysis of internal device behavior is not possible, thus preventing a thorough understanding of the processes involved. The work presented here enables us to look into the details of internal device behavior under large-signal operation. We can thus assess qualitatively and quantitatively the relative merits of various device structures, biasing and loading arrangements. This understanding should prove very useful in design of devices and associated circuitry for wireless mobile handsets.

VII. CONCLUSION

An accurate, fully physical, simulator for CAD has been presented which is capable of simulating pHEMT intermodulation performance based on a description of device epitaxy and geometry. Simulated two-tone results have been presented which agree very well with measured data into gain compression of up to 4.5 dB. The authors believe that these are among the best results presented for multitone simulations using either physically derived, measurement-based, or empirical models for microwave pHEMTs. Using the model, it is possible to examine internal device behavior such as charge density or electric field variations along the channel as a function of time. We have highlighted the major contributions to distortion in HEMTs in terms of internal physical device behavior and demonstrated that the work presented allows us to investigate physical device behavior that cannot otherwise be investigated with quasistatic large-signal equivalent-circuit device models. The work presented here will facilitate a greater understanding of large-signal HEMT operation including guidelines on device design, operating points and loading.

ACKNOWLEDGMENT

The authors would like to acknowledge the assistance of Dr. A. Panks, Dr. R. Johnson, and N. Bourhill.

REFERENCES

- [1] D. E. Root, S. Fan, and J. Meyer, "Technology-independent large-signal non quasistatic FET models by direct construction from automatically characterized device data," in *Proc. 21st Eur. Microwave Conf.*, Sept. 1991, pp. 927–932.
- [2] C. G. Morton, C. M. Snowden, and M. J. Howes, "HEMT physical model for MMMIC CAD," in *Proc. 25th Eur. Microwave Conf.*, Sept. 1995, pp. 199–204.
- [3] C. G. Morton, J. S. Atherton, C. M. Snowden, R. D. Pollard, and M. J. Howes, "A large-signal physical HEMT model," in *IEEE MTT-S Int. Microwave Symp. Dig.*, June 1996, pp. 1759–1762.
- [4] C. M. Snowden and R. R. Pantoja, "GaAs MESFET physical models for process-oriented design," *IEEE Trans. Microwave Theory Tech.*, vol. 40, pp. 1401–1409, July 1992.
- [5] R. Drury and C. M. Snowden, "A quasi-two-dimensional HEMT model for microwave CAD applications," *IEEE Trans. Electron Devices*, pp. 1026–1032, June 1995.
- [6] K. Gard, H. Gutierrez, and M. B. Steer, "Characterization of spectral regrowth in microwave amplifiers based on the nonlinear transformation of a complex Gaussian process," *IEEE Trans. Microwave Theory Tech.*, vol. 47, pp. 1059–1069, July 1999.

- [7] C. M. Snowden and R. R. Pantoja, "Quasi-two-dimensional MESFET simulations for CAD," *IEEE Trans. Electron Devices*, vol. 36, pp. 1564–1574, Sept. 1989.
- [8] C. G. Morton and C. M. Snowden, "Comparison of quasi-2D and ensemble Monte Carlo simulations for deep submicron HEMTs," in *IEEE MTT-S Int. Microwave Symp. Dig.*, vol. 1, 1998, pp. 153–156.
- [9] P. Sandborn, A. Rao, and P. Blakey, "An assessment of approximate nonstationary charge transport models used in GaAs device modeling," *IEEE Trans. Electron Devices*, vol. 36, pp. 1244–1253, July 1989.
- [10] C. G. Morton and C. M. Snowden, "Quasi-two dimensional modeling of HEMTs," in *Proc. 8th GaAs Simulation Workshop*, Oct. 1994.
- [11] S. A. Maas, *Nonlinear Microwave Circuits*. Norwood, MA: Artech House, 1988.
- [12] T. Shawki, G. Salmer, and O. El-Sayed, "MODFET 2-D hydrodynamic energy modeling: Optimization of subquarter-micron-gate structures," *IEEE Trans. Electron Devices*, vol. 37, pp. 21–30, Jan. 1990.
- [13] J. Wood and C. G. Morton, "An analysis of the effective position of the two-dimensional electron gas in the channel of MODFET epitaxial layer structures," *IEEE Trans. Electron Devices*, vol. 45, pp. 1622–1624, July 1998.
- [14] R. E. Williams and D. W. Shaw, "Graded channel FETs: Improved linearity and noise figure," *IEEE Trans. Electron Devices*, vol. ED-25, pp. 600–605, June 1978.
- [15] J. C. Pedro, "Evaluation of MESFET nonlinear intermodulation distortion reduction by channel-doping control," *IEEE Trans. Microwave Theory Tech.*, vol. 45, pp. 1989–1997, Nov. 1997.
- [16] R. A. Pucel, "Profile design for distortion reduction in microwave field-effect transistors," *Electron. Lett.*, vol. 14, pp. 204–206, Mar. 1978.
- [17] J. A. Higgins and R. L. Kuvas, "Analysis and improvement of intermodulation distortion in GaAs power FETs," *IEEE Trans. Microwave Theory Tech.*, vol. MTT-28, pp. 9–17, Jan. 1980.
- [18] W. S. Lour, H. R. Chen, and L. T. Hung, "Low distortion AlGaAs/InGaAs power HFET's with quantum-doped graded-like channels," *Semiconduct. Sci. Technol.*, vol. 12, no. 10, pp. 1210–1216, 1997.
- [19] Z. Borsosfoldi, D. R. Webster, I. G. Thayne, A. Asenov, D. G. Haigh, and S. P. Beaumont, "Ultra-linear pseudomorphic HEMT's for wireless communications: A simulation study," *Inst. Phys. Conf. Series*, vol. 156, pp. 475–478, 1997.

Peter J. Rudge received the M.Eng. degree in electronic engineering from The University of Leeds, Leeds, U.K., in 1998, and is currently working toward the Ph.D. degree at The University of Leeds, where his work, which is being conducted in association with M/A-COM Corporate R&D, has involved the utilization of a physical pHEMT model to investigate nonlinear transistor behavior.

In particular, his research is concerned with the physical simulation of pHEMT structures with a view to minimizing intermodulation distortion and spectral regrowth in power amplifiers for digital wireless communications.

Robert E. Miles received the Ph.D. degree from the University of London, London, U.K., in 1972.

He began his research in 1964 with Zenith Radio Research (UK) Ltd., where he was involved with compound semiconductors. After a period as a School Teacher, he joined the Department of Electronic and Electrical Engineering, The University of Leeds, Leeds, U.K., as a Research Engineer to work on III–V semiconductors. He joined the University of Bradford for two years before returning to The University of Leeds, where he is currently a Reader in Semiconductor Materials and Devices. His research interests include the fabrication of Gunn diodes, HEMTs, HBTs, resonant tunnelling diodes, and thin-film piezo-ceramic layers on GaAs. He is a member of the UK TINTIN Group, which is involved with terahertz frequency devices and circuits. He co-organized the NATO ASI on "New Direction in Terahertz Technology" in 1996, and also the NATO ARW entitled "Terahertz Sources and Systems" in 2000. He is a member of the European "INTERACT" terahertz group. He has recently extended his interests into optically generated terahertz systems, and is a member of the Teravision Project, sponsored by the European Union.

Michael B. Steer (S'76–M'78–SM'90–F'99) received the B.E. and Ph.D. degrees in electrical engineering from the University of Queensland, Brisbane, Australia, in 1976 and 1983, respectively.

He is currently a Professor of electrical and computer engineering at North Carolina State University, Raleigh. His research work has been closely tied to solving fundamental problems in modeling and implementing RF and microwave circuits and systems. Up to 1996, he was the founding Librarian of the IBIS Consortium, which provides a forum for developing behavioral models. A converter written by his group to automatically develop behavioral models from a SPICE netlist (*spice2ibis*) is being used throughout the digital design community. Currently, one of his interests is in global modeling of the physical layer of RF, microwave, and millimeter-wave electronic systems in support of multifunctional adaptive RF frontends. He is performing research in technology integration, as well as signal integrity and circuit modeling in general. In 1999 and 2000, he was a Professor in the School of Electronic and Electrical Engineering, The University of Leeds, where he held the Chair in Microwave and Millimeterwave Electronics. He was also Director of the Institute of Microwaves and Photonics, The University of Leeds. He has organized many workshops and taught many short courses on signal integrity, wireless, and RF design. He has authored or co-authored over 200 refereed papers and book chapters on topics related to high-speed digital design and RF and microwave design methodology. He co-authored *Foundations of Interconnect and Microstrip Design* (New York: Wiley, 2000).

Prof. Steer is active in the IEEE Microwave Theory and Techniques Society (IEEE MTT-S). In 1997, he was secretary of the IEEE MTT-S, and from 1998 to 2000, was an elected member of its Administrative. He is a 1987 Presidential Young Investigator (USA), and in 1994, and again in 1996, he was awarded the Bronze Medallion by U.S. Army Research for his Outstanding Scientific Accomplishment.

Christopher M. Snowden (S'82–M'82–SM'91–F'96) received the B.Sc. (with honors), M.Sc., and Ph.D. degrees from The University of Leeds, Leeds, U.K.

After graduating in 1977, he was an Applications Engineer for Mullard, near London, U.K. (now part of Philips). His Ph.D. studies were later conducted in association with Racal-MESL and were concerned with the large-signal characterization and design of MESFET microwave oscillators. He has held the personal Chair of Microwave Engineering at The University of Leeds since 1992. From 1995 to 1998, he was Head of the Department, and subsequently Head of the School of Electronic and Electrical Engineering. He was the first Director of the Institute of Microwaves and Photonics, The University of Leeds. He was a consultant to M/A-COM Inc. from 1989 to 1998. In 1998, he joined Filtronic, as Director of Technology. His main personal research interests include semiconductor device and circuit modeling (CAD), and microwave, millimeter-wave, and optoelectronic circuit technology. He is currently Joint Chief Executive of Filtronic plc and Professor of Microwave Engineering at The University of Leeds. His main research interests include compound semiconductor device modeling, microwave, terahertz and optical nonlinear subsystem design, and advanced semiconductor devices. He has authored eight books, over 250 refereed journal and conference papers, and many other papers.

Prof. Snowden is a Fellow of the Royal Academy of Engineering and the Institution of Electrical Engineers. He is currently a Distinguished Lecturer for the IEEE (Electron Devices Society). He was the recipient of the 1999 Microwave Prize presented by the IEEE Microwave Theory and Techniques Society (IEEE MTT-S).